Memoirs of the School of Engineering, Okayama University, Vol. 15-2, March 1981

Dynamical Fluctuation Spectra of Two-Dimensional Classical Electron Liquids

Hiroo TOTSUJI*, Takashi OBATA*, and Takahiko FUNAHASHI*

(Received February 7, 1981)

Synopsis

The dynamic form factor and the transverse part of the fluctuation spectrum of momentum density are analysed on the basis of the generalized Langevin equation. According to the indication of the result, numerical experiments are extended and it is shown that the transverse fluctuation spectrum contains two kinds of excitations. The frequency moment sum rules are discussed in relation to one of these excitations.

1. Introduction

The one-component plasma (OCP, the system of charged particles in a uniform neutralizing background) is a simple and typical example of classical liquid with long-range interactions and various investigations have been made on both static and dynamic properties [1]. In the domain of strong coupling where we have no small parameter to expand physical quantities, the results of "exact" numerical experiments are of fundamental importance as the basis of theoretical works.

Since the two-dimensional classical electron liquid shares basic properties with the OCP in three dimensions and is, at present, the only possibility of realizing the OCP in a laboratory experiment, there has been a growing interest in this system. The dynamic

* Department of Electronics

properties of strongly coupled electron liquids in two dimensions have been obtained by numerical experiments [2]: The longitudinal fluctuation spectrum is characterized by the collective excitation (the plasma oscillation) with the dispersion relation interpolating the one in dilute plasmas and the one in the Wigner lattice, and the transverse spectrum, by the existence of the shear mode in the domain of relatively large wave numbers. Compared with the case of three dimensions [3], the behavior of the transverse spectrum is different in that there is a domain of wave numbers where the excitation has a pronounced single peak structure; the transverse excitation appears as a double peak in three dimensions.

The purpose of this paper is to analyse these dynamic spectra of two-dimensional electron liquids on the basis of the Mori generalized Langevin equation and to clarify the nature of transverse excitations in the domain of strong coupling.

The two-dimensional electron liquid is characterized by the dimensionless parameter Γ defined by $\Gamma = (\pi n)^{1/2} e^2/T$, where n, e, and T are the number density, the electronic charge, and the temperature in energy units. This parameter represents the strength of the Coulomb interaction relative to the average kinetic energy: The system is a weakly coupled plasma, a liquid of intermediate or strong coupling, and the Wigner lattice, when $\Gamma \lesssim 1$, $1 \lesssim \Gamma \lesssim 135$, and $135 \lesssim \Gamma$, respectively. (There is no phase transition between the gas and liquid states.) In this paper, we consider the domain of strongly coupled liquid.

2. Phenomenological Analyses of Fluctuation Spectra

The spectrum of density fluctuations, the dynamic form factor $S(k,\omega)$, and the spectrum of momentum density fluctuations, $\underset{\approx}{C}(\underset{\sim}{k},\omega)$, are defined by

$$S(k,\omega) = \frac{1}{2\pi}\int_{-\infty}^{\infty} dt \exp(i\omega t) \Big\langle \sum_{i,j} \rho^i_{\underset{\sim}{k}}(t) \rho^j_{-\underset{\sim}{k}}(t=0) \Big\rangle, \tag{2.1}$$

$$\underset{\approx}{C}(\underset{\sim}{k},\omega) = \frac{1}{2\pi}\int_{-\infty}^{\infty} dt \exp(i\omega t) \Big\langle \sum_{i,j} g^i_{\underset{\sim}{k}}(t) g^j_{-\underset{\sim}{k}}(t=0) \Big\rangle, \tag{2.2}$$

where

$$\rho^{i}_{\underset{\sim}{k}}(t) = \exp[-i\underset{\sim}{k}\cdot\underset{\sim}{r}_i(t)], \tag{2.3}$$

$$\underset{\sim}{g}^{i}_{\underset{\sim}{k}}(t) = (d\underset{\sim}{r}_i(t)/dt)\exp[-i\underset{\sim}{k}\cdot\underset{\sim}{r}_i(t)], \tag{2.4}$$

and $< >$ denotes the statistical average. Due to isotropy of our system, $\underset{\approx}{C}(\underset{\sim}{k},\omega)$ is divided into the longitudinal and the transverse parts, $C_\ell(k,\omega)$ and $C_t(k,\omega)$, as

$$\underset{\approx}{C}(\underset{\sim}{k},\omega) = (\underset{\sim}{k}\underset{\sim}{k}/k^2)C_\ell(k,\omega) + (\underset{\approx}{I} - \underset{\sim}{k}\underset{\sim}{k}/k^2)C_t(k,\omega), \tag{2.5}$$

and $C_\ell(k,\omega)$ is related to $S(k,\omega)$ by

$$k^2C_\ell(k,\omega) = \omega^2S(k,\omega). \tag{2.6}$$

These dynamic spectra have been obtained by molecular-dynamics numerical experiments [2]; their characteristic features are briefly mentioned in Section 1.

Since we have no established first-principle approaches to dynamical behaviors of strongly coupled liquids, we here make a phenomenological analysis employing the generalized Langevin equation due to Mori [4].

The Liouville equation for a dynamical quantity $A(t)$ can be rewritten into the form

$$dA(t)/dt - i\Omega A(t) + \int_0^t ds\, M(t-s)A(s) = R(t). \tag{2.7}$$

Here the frequency Ω describes the relaxation proportional to $A(t)$, the memory effect is expressed by $M(t)$, and $R(t)$ denotes the random force which is orthogonal (uncorrelated) to $A(t=0)$. Noting that the random force $R(t)$ obeys an equation similar to (2.7), we arrive at the continued fraction representation of the dynamical behavior of fluctuations [4].

For the dynamic form factor, the continued fraction representation to the third order reads

$$S(k,\omega) = [NS(k)/\pi]\mathrm{Re}[1/(-i\omega + \Delta_1^2/(-i\omega+\Delta_2^2/(-i\omega + \Delta_3^2\tilde{M}(k,\omega))))]. \tag{2.8}$$

Here N is the number of particles in our system, S(k) the static form factor

$$S(k) = \langle \rho_{\underset{\sim}{k}}(t)\rho_{-\underset{\sim}{k}}(t)\rangle/N, \tag{2.9}$$

and $\tilde{M}(k,\omega)$ is the Laplace transform of the memory function M(k,t) which is normalized as M(k,t=0)=1. The coefficients Δ_n^2 are related to the frequency moments of $S(k,\omega)$ as

$$\Delta_1^2 = \langle\omega\rangle/\langle\omega^{-1}\rangle, \tag{2.10}$$

$$\Delta_2^2 = \langle\omega^3\rangle/\langle\omega\rangle - \Delta_1^2, \tag{2.11}$$

$$\Delta_3^2 = (\langle\omega^5\rangle/\Delta_1^2 - \langle\omega^3\rangle)/\langle\omega^{-1}\rangle\Delta_2^2 - \Delta_1^2 - \Delta_2^2, \tag{2.12}$$

where

$$\langle\omega^m\rangle = \frac{1}{\pi}\int_{-\infty}^{\infty} d\omega\omega^{m+1}S(k,\omega). \tag{2.13}$$

As the memory function, the Gaussian or the exponential decay is commonly used in this kind of analyses. We also adopt

$$M(k,t) = \exp[-f(k)t^2] \tag{2.14}$$

or

$$M(k,t) = \exp[-f(k)t] \tag{2.15}$$

as a simple trial function.

Using Eqs.(2.8) ∿ (2.15), we determine the parameter f(k) included in the memory function so as to reproduce the experimental results. We have also checked the consistency of experimental values of the dynamic form factor comparing the frequency moments up to m=3 with the

values computed from static correlation functions by frequency moment sum rules. Some examples of the dynamic form factor are shown in Figs.1(a)∿1(e).

The results of comparisons of Eq.(2.8) with experimental values of dynamic form factor may be summarized as follows: (a) The dynamic form factor can be reproduced by Eq.(2.8) with the Gaussian memory function (2.14), (b) f(k) is roughly equal to $\omega_p^2(\sqrt{\pi n})=(2\pi ne^2\sqrt{\pi n}/m)$ (m being the electronic mass) and slightly increases with the wave number k, and (c) the difference between Eq.(2.8) and experimental values becomes significant in the domain of large wave numbers where the longitudinal excitation has a broad peak structure.

The continued fraction representation for the transverse part of the momentum density fluctuations is given by

$$C_t(k,\omega) = (NT/\pi m)\mathrm{Re}[1/(-i\omega + \Delta_1^2/(-i\omega + \Delta_2^2\tilde{M}(k,\omega)))], \tag{2.16}$$

where

$$\Delta_1^2 = (m/N)\langle\omega\rangle_t, \tag{2.17}$$

$$\Delta_2^2 = \langle\omega^3\rangle_t/\langle\omega\rangle_t - \Delta_1^2, \tag{2.18}$$

$$\langle\omega^m\rangle_t = \frac{1}{T}\int_{-\infty}^{\infty} d\omega\omega^{m+1}C_t(k,\omega). \tag{2.19}$$

In Figs.2(a)∿2(e), we show some examples of the values of Eq.(2.16) with Eq.(2.14) as M(k,t) in comparison with experimental values. The results of the continued fraction representation are not so satisfactory as in the case of longitudinal spectrum, especially in the domain of relatively large wave numbers where pronounced but rather broad peak appears.

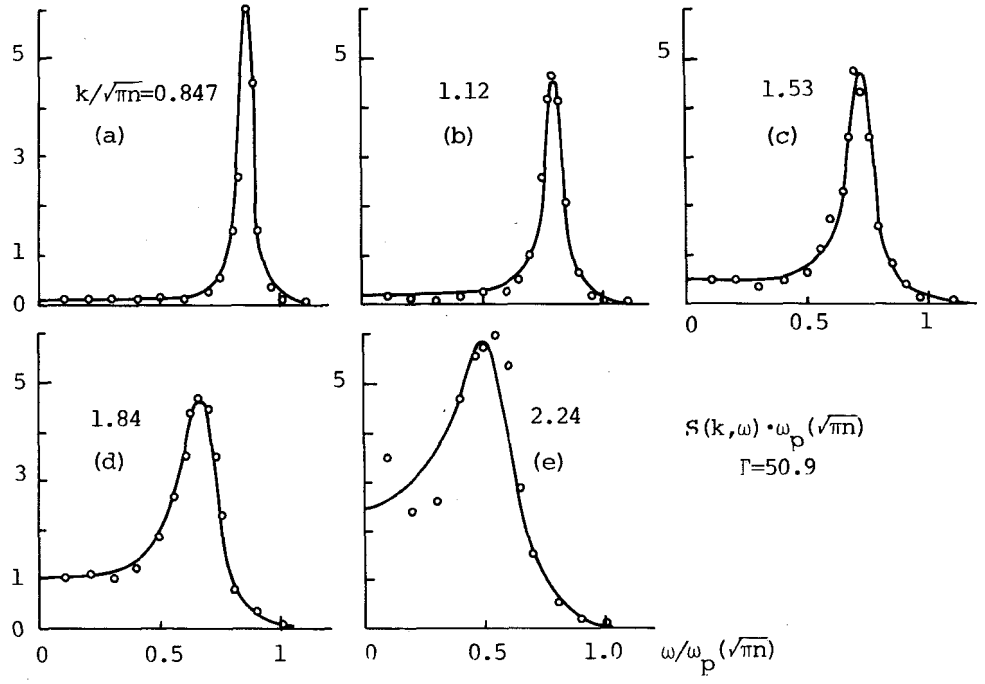

Fig.1. The dynamic form factor $S(k,\omega)$ for $\Gamma\tilde{=}51$. Open circles are experimental values and solid lines represent those given by Eqs.(2.8) and (2.14). The memory function (2.15) gives the results which decay more rapidly on the high frequency side.

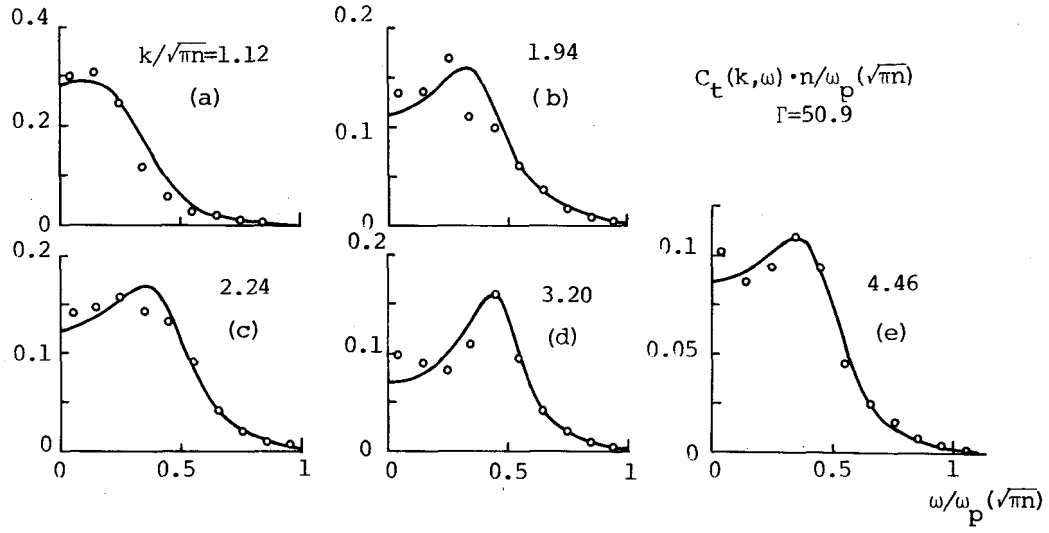

Fig.2. The transverse fluctuation spectrum $C_t(k,\omega)$ of the momentum density for $\Gamma\tilde{=}51$. Open circles are experimental values and solid lines are those given by Eqs.(2.14) and (2.16). The memory function (2.15) gives shorter high frequency tails.

3. Structure of Transverse Fluctuation Spectrum

In the case of strongly coupled OCP in three dimensions, the transverse spectrum has the double peak structure and a theoretical explanation of this structure has been given by a mode-coupling theory [5]. Previous analysis of the transverse spectrum in two-dimensional electron liquids was not conclusive on this point due to statistical errors [2].

On the other hand, a phenomenological analysis of this spectrum in Section 2 seems to indicate the necessity of introducing another concept in the domain of large wave numbers. We therefore have extended previous numerical experiments and obtained the transverse spectrum based on almost tripled data.

Resultant spectra are plotted for $\Gamma \cong 50$ and $\Gamma \cong 70$ in Figs.3(a) and 3(b) where statistical errors are also shown. We see the appearance of an excitation of apparently different nature from that of small wave numbers.

The change of the transverse spectrum with increasing wave number may be summarized as follows: (a) In the long-wavelength domain $k/(\pi n)^{1/2} \lesssim 1$, the spectrum is diffusive, (b) a shoulder appears at the wave number around $(\pi n)^{1/2}$ and grows with the wave number, (c) another excitation with higher frequency appears around $k/(\pi n)^{1/2} \sim 2.2$, (d) the latter excitation becomes pronounced while the former disappears, and (e) the spectrum returns to a diffusive one for $5 \lesssim k/(\pi n)^{1/2}$.

In order to clarify the origin of transverse excitations for large wave numbers, we note that the spectrum $C_t(k,\omega)$ is divided into the coherent and the incoherent parts, $C_t^{coh}(k,\omega)$ and $C_t^{inc}(k,\omega)$, as

$$C_t(k,\omega) = C_t^{coh}(k,\omega) + C_t^{inc}(k,\omega) \geq 0, \tag{3.1}$$

$$C_t^{inc}(k,\omega) = \frac{1}{2\pi}\int_{-\infty}^{\infty} dt \exp(i\omega t) < \sum_{i=1}^{N} \cdots > \geq 0, \tag{3.2}$$

$$C_t^{coh}(k,\omega) = \frac{1}{2\pi}\int_{-\infty}^{\infty} dt \exp(i\omega t) < \sum_{i \neq j} \cdots >. \tag{3.3}$$

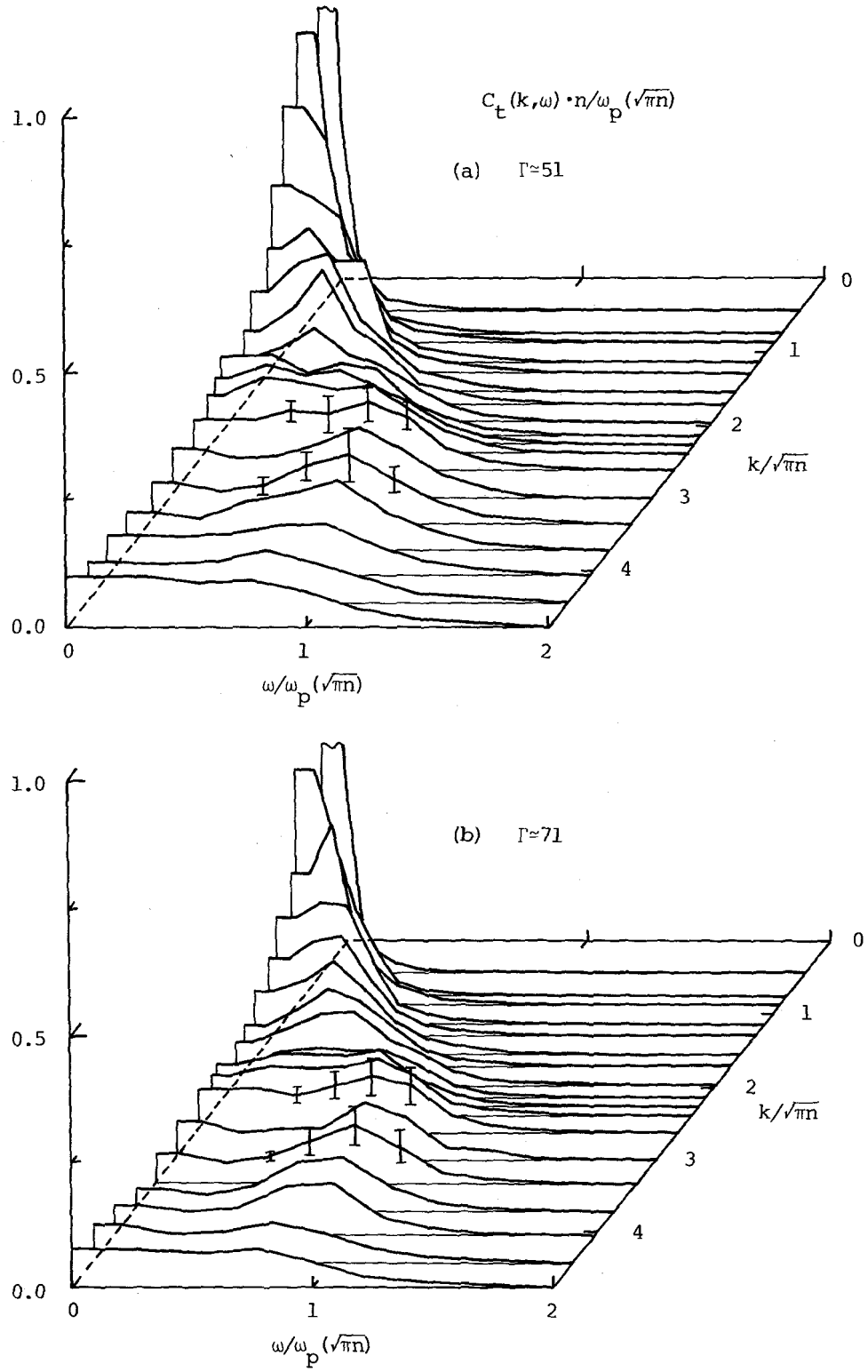

Fig.3. The transverse fluctuation spectrum $C_t(k,\omega)$ of the momentum density for $\Gamma\simeq 51$ and $\Gamma\simeq 71$.

The sum rules for corresponding frequency moments are given by

$$\langle\omega^{-1}\rangle_t^{inc} = N/m, \tag{3.4}$$

$$\langle\omega\rangle_t^{inc} = (N/m)k^2(T/m) + (N/m)(ne^2/2m)\int d\underset{\sim}{r}\, g(r)/r^3, \tag{3.5}$$

$$\langle\omega^{-1}\rangle_t^{coh} = 0, \tag{3.6}$$

$$\langle\omega\rangle_t^{coh} = -(N/m)(ne^2/2m)\int d\underset{\sim}{r}\, g(r)[J_0(kr) + 3J_2(kr)]/r^3, \tag{3.7}$$

where $g(r)$ is the pair distribution function and $J_n(x)$ is the Bessel function of n-th order.

In Fig.4 we plot the values of each contribution to $\langle\omega\rangle_t^{inc}$ and $\langle\omega\rangle_t^{coh}$ computed from the results of Monte Carlo experiments [6].

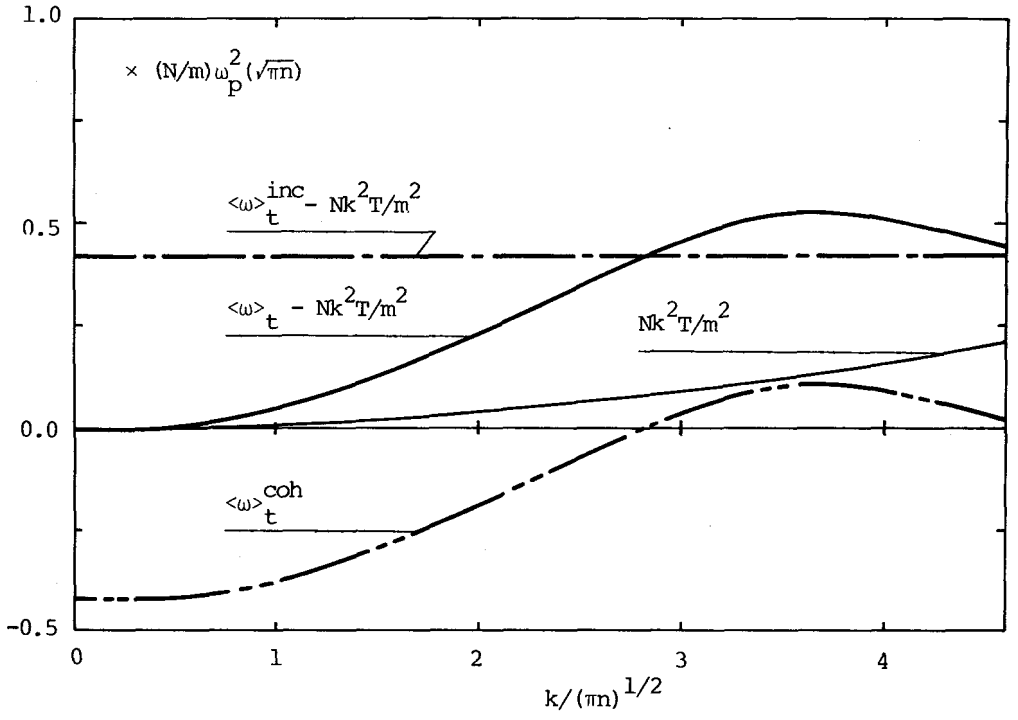

Fig.4. Coherent and incoherent contributions to the first frequency moment $\langle\omega\rangle_t$ of the transverse spectrum for $\Gamma\cong 51$.

Note that, in the domain $3 \leq k/(\pi n)^{1/2}$ where the pronounced single peak appears, most part of the value of $\langle\omega\rangle_t$ comes from the incoherent part $\langle\omega\rangle_t^{inc}$. Though the coherent part $C_t^{coh}(k,\omega)$ is not positive (or negative) definite as a function of ω, small values of $\langle\omega\rangle_t^{coh}$ and Eq.(3.6) indicate that the absolute value of $C_t^{coh}(k,\omega)$ is much smaller than $C_t^{inc}(k,\omega)$:

$$C_t(k,\omega) \cong C_t^{inc}(k,\omega) \qquad \text{for} \qquad 3 \leq k/(\pi n)^{1/2}. \tag{3.8}$$

Because $C_t^{inc}(k=0,\omega)$ reduces to the velocity autocorrelation function $C_v(\omega)$ as

$$C_t(k=0,\omega) = (N/2)C_v(\omega), \tag{3.9}$$

$$C_v(\omega) = \frac{1}{2\pi}\int_{-\infty}^{\infty} dt \exp(i\omega t)\langle g^i_{\underset{\sim}{k}=0}(t)\cdot g^i_{\underset{\sim}{-k}=0}(t=0)\rangle, \tag{3.10}$$

we expand $C_t^{inc}(k,\omega) - (N/2)C_v(\omega)$ as

$$C_t^{inc}(k,\omega) - (N/2)C_v(\omega) \cong Ak^2 \tag{3.11}$$

$$Ak^4 = -(N/4\pi)\int_{-\infty}^{\infty} dt \exp(i\omega t)\langle [\underset{\sim}{k}\times g^i_{\underset{\sim}{k}=0}(t)]\cdot[\underset{\sim}{k}\times g^i_{\underset{\sim}{-k}=0}(0)]\{\underset{\sim}{k}\cdot[\underset{\sim}{r}_i(t)-\underset{\sim}{r}_i(0)]\}^2\rangle. \tag{3.12}$$

The coefficient A may be estimated by considering two limiting cases where $C_v(\omega)$ is peaked around $\omega=0$ and peaked around $\omega_0 \sim \omega_p(\sqrt{\pi n})$. In the former, we estimate $\{\underset{\sim}{k}\cdot[\underset{\sim}{r}_i(t)-\underset{\sim}{r}_i(0)]\}^2$ by $k^2(T/m)t^2$ and have

$$|Ak^2| \sim k^2(T/m)\,|\partial^2 C_v(\omega)/\partial\omega^2| \ll C_v(\omega) \tag{3.13}$$

when $k(T/m)^{1/2} \ll \omega$. In the latter, we rewrite $\{\underset{\sim}{k}\cdot[\underset{\sim}{r}_i(t)-\underset{\sim}{r}_i(0)]\}^2$ as $(T/m)\omega_0^{-2}\cos^2\omega_0 t$ and obtain

$$|Ak^2| \lesssim k^2(T/m)\omega_0^{-2}\mathrm{Max}[C_v(\omega\pm\omega_0), C_v(\omega)] \ll C_v(\omega) \tag{3.14}$$

when $k^2(T/m) << \omega_0^2 \sim \omega_p^2(\sqrt{\pi n})$. Since

$$k^2(T/m)/\omega_p^2(\sqrt{\pi n}) = (k^2/\pi n)/2\Gamma \tag{3.15}$$

and therefore

$$|Ak^2| << C_v(\omega) \tag{3.16}$$

for

$$k/(\pi n)^{1/2} \lesssim 4 \qquad \text{and} \qquad \Gamma \gtrsim 50 \tag{3.17}$$

in both limiting cases, we may have

$$C_t^{inc}(k,\omega) \simeq (N/2)C_v(\omega) \tag{3.18}$$

in the domain (3.17).

Eq.(3.18) indicates that the structure of the incoherent spectrum in the domain of long wavelengths persists up to relatively short wavelengths. Thus the spectrum of the velocity autocorrelation function coupled mainly to well-defined longitudinal oscillation can appear as the incoherent transverse spectrum of large wave numbers.

We may thus have an interpretation of the behavior of transverse spectrum: A collective shear mode exists only up to the wave number around $2(\pi n)^{1/2}$ and the peak structure for larger wave numbers is due to single-particle motion which is driven by the longitudinal collective mode.

Obtained separately, the coherent and the incoherent parts of longitudinal and transverse spectra contain useful information not only for the problem considered here but also for other theoretical investigations. The analyses in this direction are now in progress.

Acknowledgements

Numerical computations have been mainly done at the Okayama University Computer Center. The authors wish to thank Professor

Y. Furutani for his interest in the work. This work has been partially supported by the Grant-in-Aids for Scientific Researches of the Ministry of Education.

References

[1] For example, M. Baus and J. P. Hansen : Phys. Reports 59(1980), 1.

[2] H. Totsuji and H. Kakeya : Phys. Rev. A22(1980), 1220.

[3] J. P. Hansen, I. R. McDonald, and E. L. Pollock : Phys. Rev. Lett. 32(1974), 277; Phys. Rev. A11(1975), 1025.

[4] H. Mori : Progr. Theor. Phys. 33(1965), 423; ibid. 34(1965), 399.

[5] J. Bosse and K. Kubo : Phys. Rev. Lett. 40(1978), 1660; Phys. Rev. A18(1978), 2337.

[6] H. Totsuji : Phys. Rev. A17(1978), 399.